A High Spatiotemporal Chemical Shift Imaging Technique for MR-Guided Thermal Therapy with Multi-Parametric Monitoring Capabilities

B. A. Taylor[1], K-P. Hwang[1,2], A. M. Elliott[1], A. Shetty[1], J. D. Hazle[1], and R. J. Stafford[1]

[1]Imaging Physics, The University of Texas M.D. Anderson Cancer Center, Houston, Texas, United States, [2]GE Healthcare Technologies, Waukesha, Wisconsin, United States

Introduction

Magnetic resonance temperature imaging (MRTI) can potentially monitor thermal therapy procedures through the measurement of the proton resonant frequency (PRF) shift (1). Currently the two most established techniques for measuring PRF are complex phase-difference (CPD) (2) and chemical shift imaging (CSI) (3) techniques. CPD techniques have been the most commonly used since it facilitates mapping of tissue temperature changes with a high spatiotemporal resolution of 1.5x1.5x3 mm^3 with imaging times of five seconds or less (4). However, they are susceptible to artifacts arising from intravoxel lipid contamination, inter- and intra-scan motion, local susceptibility changes and static magnetic field drifts. CSI techniques can, in many instances, alleviate artifacts seen in the CPD techniques (3), but their poor spatiotemporal resolution has limited its routine use for monitoring rapid thermal therapy procedures. In this work, we present a CSI technique with spatial, temporal, and temperature resolutions that are comparable to CPD techniques while still providing the advantages of a CSI-based approach to MRTI. This technique takes a novel approach to frequency estimation for temperature measurements via autoregressive moving average (ARMA) modeling (5) to overcome limitations seen in low spectral resolution, Fourier-based frequency estimation methods. Also, additional measurements such as T1 and R2* can be simultaneously acquired with the PRF to facilitate a multi-parametric approach to temperature imaging.

Methods

A 2D, multiple, fast gradient echo (MFGRE) acquisition was utilized on 1.5T and 3T clinical MR scanners (GE Healthcare, Waukesha, WI) to obtain data for 2D temperature mapping. The PRF of water and lipid were calculated through autoregressive moving average (ARMA) modeling which can extract the frequencies and R2* values of each chemical species (i.e. water, lipid) by assuming a linear combination of complex exponentials with Gaussian noise. The amplitude of each of the chemical species was calculated using Cauchy's Calculus of Residues theorem (6). To demonstrate the feasibility of this technique, phantom (1.5T), *ex vivo* (3T), and *in vivo* (1.5T) experiments were performed. The temperature sensitivity coefficient of a water-lipid phantom was calculated and compared to published literature (7). Parallel imaging (ASSET) was implemented with an acceleration factor of 2. Other acquisition parameters were: ETL=16; ESP=3.3 ms; TR=140 ms; FA=60º; rBW=325 Hz/pixel, acquisition matrix=256x128; voxel volume=0.78x1.6x3.0 mm^3; acquisition time=10 sec (for calibration purposes). Laser heating was monitored in *ex vivo* bone marrow in a canine femur at 3T to demonstrate the use of the lipid reference to correct for drift and susceptibility (ETL=16; ESP=1.8 ms; TR=68; FA=40°; rBW=325 Hz/pixel, acquisition matrix=128x128; voxel volume=1.6x1.6x5.0 mm^3; 5 sec/image) shown in figures 1 and 2. *In vivo* feasibility was demonstrated via interstitial laser ablation in canine prostate (ETL=16; ESP=3.2 ms; TR=69; FA=30°; rBW=244 Hz/pixel, acquisition matrix=128x128; voxel volume=1.8x1.8x4.0 mm^3; 5 sec/image) shown in figure 3. Noise measurements defined by the standard deviation of the frequency estimates were made in a 16 pixel ROI in muscle where no heating occurred. Finally, a balb/c mouse with injected nanoshells was treated with an internal laser between the tumor and the paraspinal muscle (ETL=16; ESP=3.5 ms; TR=68 ms; FA=30º; rBW=325 Hz/pixel, acquisition matrix=128x64; voxel volume=1.2x1.2x5.0 mm^3; 4.4 sec/image). Correlations between the sensitivity of T1 and R2* and frequency-based temperature were made to demonstrate additional temperature monitoring mechanisms using this acquisition.

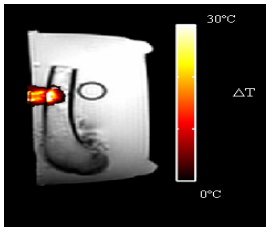

Figure 1: CSI-based temperature map of an *ex vivo* canine bone at 3T.

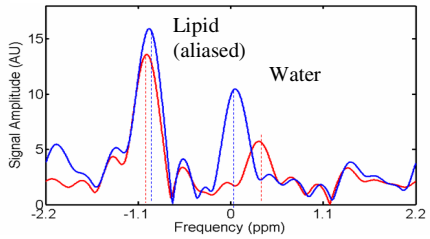

Figure 2: Spectrum of the *ex vivo* bone at room temperature (blue) and at a 25.6 °C increase (red). The solid lines represent the Fourier-based spectrum and the dashed lines represent the ARMA model calculations.

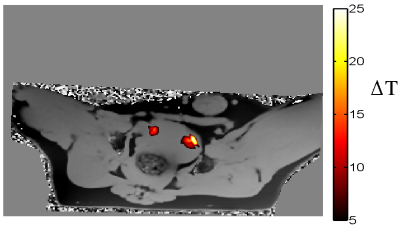

Figure 3: *In vivo* mapping of frequencies overlayed by a CSI-based temperature map in a thermal treatment of a canine prostate. The dark areas correspond to the lipid frequencies in the adipose tissue.

Results

The temperature sensitivity coefficient of the water-lipid phantom compared favorably to published literature (7). A strong linear correlation was seen in the water peak (-0.0095 ± 0.0002 ppm/°C, Pearson's R^2 = 0.996) and the difference frequencies (-0.0088 ± 0.0005 ppm/°C, Pearson's R^2 = 0.995) with less of a linear correlation seen in the lipid peak (-0.0007 ± 0.0005 ppm/°C, Pearson's R^2 = 0.530). During the heating experiment, a shift was observed due to the hot water introduced to the system to heat the phantom. This caused the mean error for the CPD and water CSI temperature readings to be 21.3 °C and 20.3 °C, respectfully. These two measurements were significantly different from the fluoroptic temperature fiber measurements ($p<0.0001$). However, when using the lipid as an internal reference the temperature remained accurate when compared to the fluoroptic fiber measurements. The mean difference between the internal reference CSI and the fluoroptic fiber was calculated to be 0.44 ± 0.34 °C. Figure 1 shows the CSI measurements of the *ex vivo* canine bone marrow 155 seconds into heating. The water and lipid signal were both easily detectable to be used in internally referenced CSI as shown in figure 2. It should also be noted that the experiment displayed the ability to monitoring the water peak separate from the lipid, which alleviates the problem of lipid contamination in PRF temperature mapping with no time or SNR penalty. Figure 3 demonstrates the ability of mapping water and lipid frequencies for MRTI *in vivo*. Noise values in the *in vivo* canine experiment were low in the frequency maps at 0.0095 ± 0.0022 ppm. The mouse *in* vivo experiment demonstrated the feasibility of using multiple parameters for temperature imaging. In T1 values had a temperature sensitivity coefficient of -1.019 ± 0.292 %/°C (Pearson's R^2 = 0.961) which is consistent with published literature (8). The R2* temperature sensitivity coefficient was -0.728 ± 0.016 %/°C (Pearson's R^2=0.788).

Conclusion

A technique is introduced which provides the benefits of a CSI approach to MRTI without sacrificing the spatiotemporal resolution achieved using standard complex phase-difference techniques. In addition to being able to use an internal lipid reference, parameters such as T1 and R2* values can be simultaneously obtained facilitating a multi-parametric approach to temperature imaging. This technique shows great promise in providing accurate temperature monitoring for minimally-invasive thermal therapies in a variety of tissues such as bone, breast and prostate.

References

1. Hindman JC. Journal of Chemical Physics 1966;44(12):4582-4592.
2. Ishihara Y, et al. Magn Reson Med 1995;34(6):814-823.
3. Kuroda K. Int J Hyperthermia 2005;21(6):547-560.
4. de Senneville BD, et al. Eur Radiol 2007;17(9):2401-2410.
5. Candy JV. Model-Based Signal Processing. John Wiley & Sons; 2006.
6. Williamson DC, et al. Magn Reson Med 2006(55); 762-771.
7. McDannold N, et al. Med Phys 2001; 28(3): 346-355.
8. Quesson B, et al. J Magn Reson Imaging 2000; 12(4): 525-533.